SAND2023-07857J

Manuscript 2/6/2023 for government review for submission to J. Electronic Materials

Radiation damage and mitigation by minority carrier injection in InAsSb/AlAsSb heterojunction barrier mid-wave infrared detector

R. E. Peale,[a,b] C. J. Fredricksen,[a] J. F. Klem,[c]

[a]Truventic LLC, Orlando FL, [b]University of Central Florida, Orlando FL, [c]Sandia National Laboratories, Albuquerque NM

ABSTRACT

Effects of gamma and proton irradiation, and of forward bias minority carrier injection, on minority carrier diffusion and photoresponse were investigated for InAsSb/AlAsSb pBn mid-wave infrared MWIR detectors with an engineered majority-carrier barrier. Room temperature gamma irradiation had insignificant effect on 77 K photoresponse. Gamma irradiation at 77 K detector temperature, however, decreased in situ photoresponse by 19% after a cumulative dose of ~500 krad(Si). Subsequent forward bias minority carrier injection had no effect on photoresponse. The 77 K detectors irradiated with 30 MeV protons up to 2 Mrad(Si) had photoresponse degraded by up to 70%, but here forward bias minority carrier (hole) injection caused up to 12% recovery that persisted more than 30 minutes. These results suggest a mitigation strategy for maintaining photoresponse of similar detectors in radiation environments that cause displacement damage defects.

Keywords: Infrared, detector, InAsSb, AlAsSb, radiation damage, proton, gamma

INTRODUCTION

Radiation damage to infrared detectors negatively impacts their space applications. For instance, devices in low-earth orbit receive ~50 krad(Si) dose per year through 2 mm of aluminum shielding, with dramatic increases during solar events [1]. Protons (from the inner van Allen belt and solar events) generate total ionizing dose (TID) and non-ionizing lattice-displacement damage. The latter creates electrically active defects, which act as recombination centers, reducing minority carrier lifetime in detector absorber layers. Proton-induced defects may also change carrier concentration [2]. Gamma irradiation is usually considered to cause mainly TID damage, but Compton electrons generated by gamma rays can also cause displacement defects [3]. Among the negative effects of radiation damage is a reduction in detector responsivity.

Detectors operating in space cannot be replaced or serviced easily. Potential defect mitigation processes such as annealing take detectors off-line and are energy consuming. It is desirable to have a means to mitigate effects of radiation damage in-situ, in real time, without taking eyes off target, requiring little energy, and which can be automated. This paper demonstrates an effect that holds promise for achieving this.

We report an in-situ process to potentially mitigate degradation of photo-response in a radiation-damaged barrier-type heterojunction mid-wave infrared detector. The detector design employs a low-doped n-type InAsSb absorber, in which photo-generated holes are minority carriers. Results reported here show that hole injection can partially restore photo-response that has been degraded by proton irradiation. Moreover, the benefit is long lasting in comparison to image-collection times. The suggested mechanism is that forward-bias hole injection restores photo-generated minority hole lifetime by passivating radiation-induced recombination centers.

Forward bias minority-carrier injection is known to provide long-lasting recovery to the photoresponse of radiation-damaged wide-gap p-i-n UV photodiodes [4,5]. UV absorption occurs in their top-most layer, which is purposely thinned to improve collection of photo-generated minority carriers since these must diffuse to the junction. Radiation damage reduces minority carrier lifetime, diffusion length, and hence quantum efficiency. Forward bias injection passivates the radiation-defect recombination centers, restoring lifetime. The benefit to photoresponse can last hours to days. This effect has been correlated with direct measurements of diffusion length by the electron-beam induced current (EBIC) technique.

Radiation damage may largely anneal out at room temperature. Indeed, no effect of room-temperature gamma radiation (522.5 krad(Si), ^{60}Co, 1.2 & 1.3 MeV) on minority carrier diffusion length in the considered detector structures was observed by EBIC [6]. This room temperature dose similarly had no effect on photoresponse [6].

Here we report photo-response measurements following gamma and proton irradiations with detectors maintained at liquid-nitrogen temperature. Photoresponse and hole-injection effects were studied without warming. Photoresponse was degraded similarly by both gamma and proton irradiation. Mitigation by forward bias hole injection occurred only after proton dosing.

Experimental Details

The MWIR detector studied was an nBp InAsSb/AlAsSb structure fabricated by Sandia National Laboratories on a GaSb substrate and designated EB3108 [7]. Figure 1 (top) presents a schematic of the layer structure. The low-doped n-type InAsSb absorber is 2 μm thick. Between the absorber and the p^+ InAsSb top contact is an AlAsSb barrier to electrons, which are majority-carriers in the absorber.

Figure 1 (bottom) presents an optical microscope image of the processed detector die with wire bonds. The multiple etched mesas of different size (490, 294, and 196 μm) have unpassivated side-walls. Some are covered completely in gold, others are windowed, and some are surrounded by guard rings. The guard rings are connected to the p^+ top layer. This material is etched away between the ring and its enclosed detector, as it is in the spaces between detectors. The detector die was mounted with indium to ceramic leadless chip carriers (LCC). Individual detectors were wire bonded to the LCC contacts.

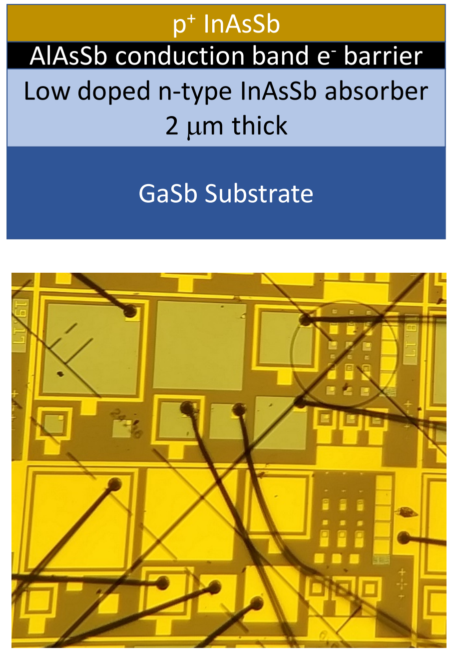

Figure 1. (top) Schematic of MWIR detector layer structure. (bottom) Microscope image of wire-bonded detectors

The LCC was snapped into a socket surface-mounted on a printed circuit board, which had been milled out to allow an aluminum cold finger to thermally contact the LCC backside via Apiezon-N grease. The cold finger was mounted to the cold plate of a liquid nitrogen cryostat, which had optical access via a 2-mm-thick ZnSe window. A platinum resistor (PT-100) embedded in the cryostat cold finger monitored temperature. Detector signals were cabled via hermetic multipin connectors to a Stanford Research SR570 current preamplifier with band-pass filtering. The output was synchronously amplified by an SR530 lock-in, whose output was recorded via LabVIEW™. Nine of the detectors on the die were monitored.

Photo-response was measured on processed detectors using a chopped blackbody source at 300 °C, whose spectrum at this temperature peaks at 5.2 μm wavelength. Photo-response spectra have been published in [6] and show a cut-off wavelength of ~4 μm. The response spectra are unaffected by room temperature gamma irradiation up to 522.5 krad(Si) [6]. In situ spectroscopic measurements were not feasible during our low-temperature irradiation experiments.

The maximum photo-response for EB3108 is achieved already at zero-bias, when the depletion width in the InAsSb absorber is ~0.15 μm [7], so measurements were performed unbiased. Forward bias minority-carrier-injection treatment was applied using a Keithley source meter. Switching between measurement and treatment was achieved via a LabVIEW™-controlled relay box. Forward bias injected current density ranged from 4 to 260 mA/mm^2. Photo-response was measured after each injection. Photo-response of untreated control detectors on the same die were simultaneously monitored.

Gamma irradiation was performed at Radiation Test Solutions (Colorado Springs) using their High Dose Rate source. Timed irradiations were performed with the cryostat window touching the housing of the retractable ^{60}Co source, where the dose rate was 50 rad(Si)/s. After the source retraction, the cryostat could be immediately removed to a photo-response/treatment test set up comprising blackbody source, chopper, preamp, lock-in amplifier, source meter, relay box, and LabVIEW computer. Photo-response was measured before and after each exposure. Forward bias injection experiments began only after significant degradation was observed.

Low temperature proton irradiations were performed at the Texas A&M University (TAMU) K150 cyclotron. The same parameters and procedures were used as in [6]. The proton beam passed through the ZnSe cryostat window before impinging on the detectors. The maximum flux was 1×10^9 protons/cm^2·s. The 30 MeV energy at the sample and the dose after each timed irradiation were determined by facility staff. At this fixed energy, absorbed dose is proportional to fluence, and an absorbed dose of 100 krad(Si) corresponds to a fluence of 5.8×10^{11} p/cm^2. The nominal range in the detector material was 4.9 millimeters, which is more than a thousand times greater than the detector epi-layer thickness.

Proton dose was controlled by exposure time at fixed flux to set the effective fluence. An accumulated dose of ~ 2 Mrad(Si) was achieved in steps while the detectors were maintained at 77 K throughout. Measurements of photo-response were interleaved with irradiation steps. A remotely-controlled off-axis parabolic flip mirror allowed the sample to view the 300 ^{o}C blackbody for photo-response measurements after each timed irradiation without moving the cryostat, giving highly repeatable optical alignment. Forward-bias injection treatments were applied after each of the two final (and largest) doses. The only physical interaction required with the setup over the course of the experiment was topping-off the cryostat reservoir with LN_2 every 2-3 hours. Solid-state relays controlled by LabVIEW and a microcontroller selected a particular detector (channel) for measurement and/or treatment. That channel's output was connected to the preamp, whose output was connected to the chopper-referenced lock-in. The mirror was flipped down to direct the output of the blackbody source onto the detectors. The DC voltage output of the lock-in was sampled at a rate of 1 Hz. Measurements were acquired for two minutes and the results averaged to obtain one value of photoresponse. To measure all channels, the switchbox cycled through the 9 detectors one after another, which took ~20 minutes to complete. Measurement times are much larger than detector thermal time constants. A measurement time of 2 minutes per detector was sufficient to establish the signal level in the presence of noise and drift, which were both about 1%.

When applying treatment (current injection), one detector was selected as the untreated control detector, and its signal was recorded. The switchbox then selected the detector to be treated, and its signal was recorded. The switchbox then connected this channel to the source meter for application of forward bias. Specified forward current was applied by the source meter for a given time. Then the treated detector's signal was remeasured, followed by a remeasurement of the control.

RESULTS

After liquid nitrogen is first added to the cryostat, the temperature sensor reaches 78 K in about 30 minutes, and the photoresponse stabilizes after about 2 hours. Irradiation and photoresponse measurements began at that time.

Figure 2 presents photoresponse vs cumulative gamma or proton dose. The photoresponse tends to scale well with detector area, and covered detectors show a reduced but non-zero response. To remove the effect of area and covering on the pre-irradiation photoresponse, the data are normalized to the value of the first measurement. Covered detectors are indicated by solid symbols and windowed detectors by open symbols. Small, medium, and large detectors are indicated by the colors black, red, and blue, respectively. Detectors with guard rings are indicated by the letter "r".

A first observation from Figure 2 is that the effect of gamma and proton irradiation is similar. Near a cumulative dose of ~700 krad(Si), the photoresponse after gamma irradiation had decreased 15 – 60%. After proton irradiation the decrease is 20 - 60% at this dose. At the highest cumulative proton dose of nearly 2 Mrad(Si), the decrease is 45 to nearly 80 %.

A second observation is that covered detectors are significantly more degraded than windowed ones. The covering is insufficient to increase damage by slowing the protons, and shielding for gammas (which would decrease damage) is also insignificant. None of the observed degradation correlates with detector size. Covered detectors with guard rings seem to suffer the most degradation, while windowed detectors with guard rings seem to suffer the least. A possible explanation for the differences is that much of the photoresponse for covered detectors arises from regions outside of the mesa by lateral diffusion of the photogenerated holes. The lateral diffusion length is long compared to the case of vertical diffusion within the mesa area. Damage that reduces the diffusion length more strongly affects this lateral-collection photoresponse mechanism more than the vertical collection process. It is difficult to predict what effect the guard rings might have, especially since they were floating and unbiased.

A third observation is that the rate of decrease in photoresponse is strongest at low dose, after which there is a tendency toward saturation of the effect. A log-log plot of the data indicates that, if each segment of the data is considered to follow a power law with negative exponent, the magnitude of that exponent is increasing with dose. At the lowest doses, the response degrades roughly as dose to the -0.03 power. At the highest dose, the exponent is about -0.5.

A fourth observation is that the photoresponse is already significantly degraded at 100 krad(Si), which contrasts with observations for nBn detectors that showed no significant change in responsivity up to that total ionizing dose [8]. We do not see the initial rise in responsivity with increasing dose up to ~ 3 krad(Si) observed in [8], which was attributed there to the effect of proton irradiation on bias. (Our first two proton doses are 1 and 5 krad(Si)). This is because for our pBn detectors, the dependence of responsivity on bias near our zero-bias operating point is small [7].

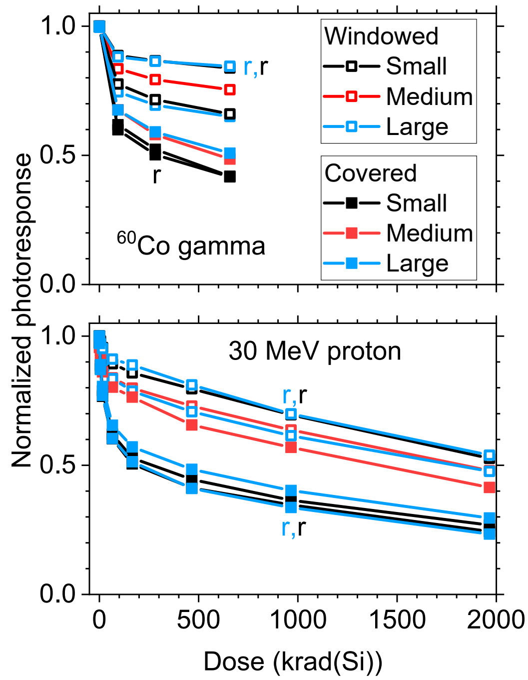

Figure 2. Photoresponse vs gamma (top) or proton (bottom) dose.

After the final gamma irradiation, a forward-bias injection treatment of 5 A-s/mm^2 minority charge was performed. No significant effect was observed. No significant difference between treated and control detectors was observed.

After each of the final two proton doses, forward bias injection treatment experiments were performed on several detectors. An untreated small ringed windowed detector was observed as the control. Its response drifted downward by about 1% per hour, and this decrease was confirmed to be common to other untreated detectors. Figure 3 presents the results. The significance of the symbol types and colors is the same as in Figure 2. The two plots represent different cumulative proton doses as indicated. The data are normalized to the signal value just before the first treatment, and they are corrected for the -1%/hr drift observed in the control detectors. The horizontal axis is injected charge per unit detector area. A first observation is that the improvement with injection was similar for identical detectors after each of the proton doses. Secondly, the benefit tends to saturate for large injected charge. Third, there does not seem to be much correlation with detector size. The largest improvement, at over 12%, was for a large windowed detector. This effect significantly exceeds the uncertainty due to either the corrected drift or noise. The smallest improvement of about 2% was also for one of the large windowed detectors, which differed from the other by having a guard ring. This improvement still significantly exceeded the uncertainty.

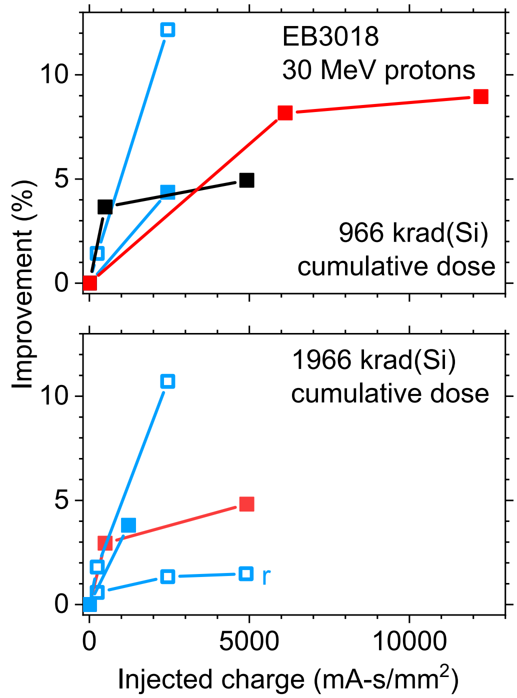

Figure 3. Improvement of photoresponse with forward bias minority carrier injection

Figure 4 presents a plot of the normalized photoresponse of the large windowed detectors as a function of time, following the maximum proton dose and a mitigation treatment that gave 11% improvement. Results are corrected for the -1%/hr drift of all control detectors during the measurements. We see that the benefit decays with a 1/e time constant of about ~30 minutes. Another forward bias injection was performed at the end of the decay experiment, and the 11% improvement was restored.

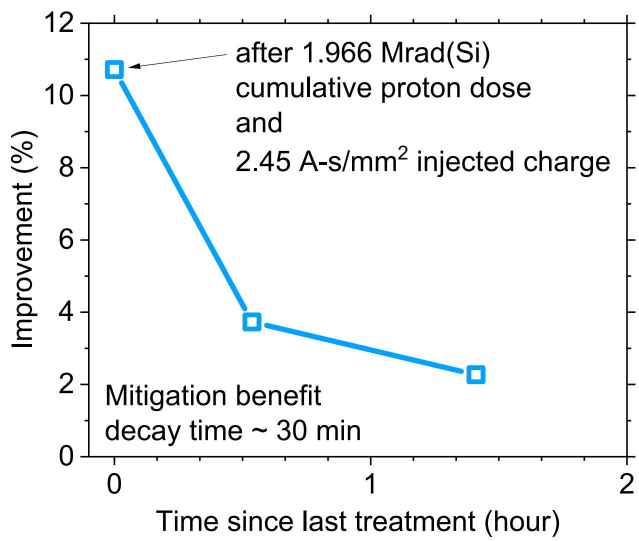

Figure 4. Persistence of Mitigation Treatment Benefit

DISCUSSION

Most of the degradation in responsivity of MWIR nBn detectors due to proton damage was attributed to reduced minority carrier lifetime in the absorber region [8,9]. Thus, a recovery of responsivity due to mitigating treatments, such as presented here for a MWIR pBn detector, might similarly be ascribed to an improvement in minority lifetime within the absorber. However, our observation in covered detectors of strong radiation damage due to protons and strong recovery due to injection suggest also a role of lateral minority carrier diffusion and passivation effects in absorber layers outside of the area covered by the top contact.

The proton damage effects reported here for 30 MeV proton energy may, in principle, be determined at other proton energies by a procedure described in [3]. Co^{60} gamma radiation, in addition to ionization-induced damage, also causes displacement damage via the ~1 MeV Compton electrons it generates [3]. We observe a very similar level of photo-response degradation at similar total ionization dose for Co^{60} irradiation as for 30 MeV protons. The reported similarity between gamma and proton dose dependence of photoresponse is not universal for different detector designs. We recently showed that an InAs/GaSb LWIR detector at 80 K showed no degradation up to a cumulative gamma dose of over 700 krad(Si), while it degraded 10% at that dose from 30 MeV protons [6].

The damage mitigation effects reported here are also not universal for different detector designs. No forward bias mitigation effect was observed in the InAs/GaSb LWIR detector at 80 K after either gamma or proton irradiation [6].

For InAs/GaSb type-II strain-layer superlattice pBp MWIR detectors that were irradiated with 63 MeV protons, response was observed to decrease linearly by up to 30% at doses up to 500 kRad(Si) [10]. This is similar to the effect we observed for uncovered pBn detectors at this dose for both gamma and proton irradiation, except the effect we observed had a non-linear dose dependence, with degradation tending to saturate.

In III-V nBn detectors, 63 MeV proton irradiation has been observed to increase the doping density of the absorber sufficiently to impact the diffusion-current and lessen its power-law-dependence on the proton fluence [2]. Such an effect may explain the saturation of photoresponse decrease that we observe at high doses. Similarly, for InAs/Ga(In)Sb type II superlattice n^+-p LWIR photodiodes irradiated with 2 MeV protons up to 2 Mrad, the p-type doping in the absorber increased with fluence [11]. Some tendency for degradation in photoresponse to saturate was observed at around 1 Mrad.

For InAs/GaSb CBIRD detectors photoresponse decreased nearly linearly up to ~14% with dose up to ~260 krad(Si) for 68 MeV protons [12]. There was only a weak tendency for the effect to saturate, in contrast to the effect reported here where saturation was already significant at this dose. Type-II antimonide superlattice infrared detectors showed no significant decrease in quantum efficiency until ~1 Mrad(Si) dose of 1 MeV protons [13], in contrast to the significant damage we observed already at 100 krad(Si) dose of 30 MeV protons in our pBn detectors. For InAs/GaSb nBn MWIR detectors, the effect of gamma irradiation on photoresponse up to 100 krad(Si) was insignificant [14], again in contrast to observations for our detectors.

CONCLUSIONS

We have demonstrated the basis for a purely electrical treatment to mitigate some of the effects of radiation damage on infrared detectors, which can be applied remotely, in situ, and autonomously for space applications. The results reported show that forward bias minority carrier injection in radiation-damaged infrared detectors fabricated with InAsSb absorbers can mitigate some of the degradation to photoresponse caused by proton irradiation damage.

ACKNOWLEDGMENTS and DISCLOSURE

REP and CJF have a financial interest in Truventic, and these authors may profit from the results of this research. This article has been coauthored by an employee JK of National Technology & Engineering Solutions of Sandia, LLC under Contract No. DE-NA0003525 with the U.S. Department of Energy (DOE). The United States Government retains and the publisher, by accepting the article for publication, acknowledges that the United States Government retains a non-exclusive, paid-up, irrevocable, world-wide license to publish or reproduce the published form of this article or allow others to do so, for United States Government purposes. This paper describes objective technical results and analysis. Any subjective views or opinions that might be expressed in the paper do not necessarily represent the views of the U.S. Department of Energy or the United States Government.

DATA AVAILABILITY

The data that support the findings of this study are available from the corresponding author upon reasonable request. The DOE will provide public access to these results of federally sponsored research in accordance with the DOE Public Access Plan https://www.energy.gov/downloads/doe-public-access-plan.

REFERENCES CITED

1. B. R. Bhat, N. Upadhyaya, and R. Kulkarni, "Total Radiation Dose at Geostationary Orbit," IEEE Trans. Nuclear Science 52, 530 (2005).
2. C.P. Morath, E.A. Garduno, G.D. Jenkins, E.A. Steenbergen, V.M. Cowan, "Effects of 63 MeV proton-irradiation on the dark-current in III-V-based, unipolar barrier infrared detectors," Infrared Physics and Technology 97, 448 (2019).
3. G. P. Summers, E. A. Burke, P. Shapiro, S. R. Messenger and R. J. Walters, "Damage correlations in semiconductors exposed to gamma, electron and proton radiations," in IEEE Trans. Nuclear Science 40, 1372 (1993).
4. O. Lopatiuk-Tirpak, L. Chernyak, L. J. Mandalapu, Z. Yang, J. L. Liu, K. Gartsman, Y. Feldman, Z. Dashevsky, "Influence of electron injection on the photoresponse of ZnO homojunction diodes," Appl. Phys. Lett., 89, 142114 (2006).

5. L. Chernyak, W. Burdett, "Electron injection-induced effects in GaN: Physics and Applications", MRS Spring Meeting Proceedings 764, C5.4 (2003).
6. C. J. Fredricksen, R. E. Peale, N. Dhakal, C. L. Barrett, T. O. Boykin II, D. Maukonen, L. Davis, B. Ferarri, L. Chernyak, O. A. Zeidan, S. D. Hawkins, J. F. Klem, Sanjay Krishna, Alireza Kazemi, Ted Schuler-Sandy, "Radiation damage and mitigation by minority carrier injection in GaSb/InAs and InAsSb/AlAsSb heterojunction barrier infrared detectors," Proc. SPIE 12107, 1210712 (2022).
7. J. F. Klem, J. K. Kim, M. J. Cich, S. D. Hawkins, T. R. Fortune, and J. L. Rienstra, "Comparison of nBn and nBp mid-wave barrier infrared photodetectors," Proc. SPIE 7608, 76081P (2010).
8. J. E. Hubbs, "Proton Radiation Experimental Results on an III-V nBn Mid-Wavelength Infrared Focal Plane Array," Proc. SPIE 9933, 993307-5 (2016).
9. C. P. Morath, V. M. Cowan, L. A. Treider, G. D. Jenkins, and J. E. Hubbs, "Proton Irradiation Effects on the Performance of III-V-Based, Unipolar Barrier Infrared Detectors," IEEE Trans. Nuclear Sci. 62, 512 (2015).
10. V. M. Cowan, C. P. Morath, J. E. Hubbs, S. Myers, E. Plis, and S. Krishna, "Radiation tolerance characterization of dual band InAs/GaSb type-II strain-layer superlattice pBp detectors using 63 MeV protons," Appl. Phys. Lett. 101, 251108 (2012).
11. E. M. Jackson, E. H. Aifer, C. L. Canedy, J. A. Nolde, C. D. Cress, B. D. Weaver, I. Vurgaftman, J. H. Warner, J. R. Meyer, J. G. Tischler, S. A. Shaw, and C. R. Dedianous, "Radiation Damage in Type II Superlattice Infrared Detectors," J. Electronic Mat. 39, 852 (2010).
12. A. Soibel, S. B. Rafol, A. Khoshakhlagh, J. Nguyen, L. Hoglund, A. M. Fisher, S. A. Keo, D. Z.-Y. Ting, and S. D. Gunapala, "Proton radiation effect on performance of InAs/GaSb complementary barrier infrared detector," Appl. Phys. Lett. 107, 261102 (2015).
13. B. D. Weaver and E. H. Aifer, "Radiation Effects in Type-Two Antimonide Superlattice Infrared Detectors" IEEE Trans. Nuclear Sci. 56, 3307 (2009).
14. V. M. Cowan, C. P. Morath, S. M. Swift, S. Myers, N. Gautam, S. Krishna, Gamma-ray Irradiation Effects on InAs/GaSb-based nBn IR Detector, Proc. SPIE 7945, 79451S (2011).